

Super Dual Auroral Radar Network observations of meteor echoes

G. E. Hall, J. W. MacDougall,¹ D. R. Moorcroft, and J.-P. St.-Maurice

Department of Physics and Astronomy, University of Western Ontario, London, Ontario, Canada

A. H. Manson and C. E. Meek

Institute for Space and Atmospheric Science, University of Saskatchewan, Saskatoon
Saskatchewan, Canada

Abstract. Radar echoes from ranges less than 500 km are routinely observed by the Super Dual Auroral Radar Network (SuperDARN) on most days. Many of these echoes have properties which are markedly different from what one would expect from *E* or *F* region irregularities. We show that these unusual short-range HF echoes are due to scattering off meteor trails. This explains why, among other things, the Doppler shift from the short-range echoes taken from the SuperDARN Saskatoon antenna are consistent with the mesospheric winds observed by the Saskatoon MF radar. This means that the SuperDARN radars can be used to study neutral winds at meteor heights, a result which is especially interesting since it opens up the capability for a global coverage of mesospheric winds using the worldwide distribution of SuperDARN radars.

1. Introduction

The Super Dual Auroral Radar Network (SuperDARN) radars provide an extensive array of auroral radars located in both the northern and southern auroral regions. Thus far, the types of echoes that have been discussed have included scattering from plasma waves in the *E* and *F* regions and ground scatter from rays totally reflected from the ionosphere [Greenwald *et al.*, 1995]. We show here that there is a third type of highly coherent echoes occurring at the near ranges (less than 400 km) which appear to be a distinctly different type of echo from those previously studied. Although *E* region auroral backscatter and possibly ground backscatter are sometimes seen at these ranges, depending on ionospheric conditions, these highly coherent echoes are observed more frequently than any other type at these ranges and are a regular daily feature of the SuperDARN radar measurements. As will be explained in more detail later, these echoes have a characteristic "grainy" appearance, due to the fact that echo intensity varies unpredictably from one range gate and integration period to the next. For convenience, we will refer to these as "grainy near-range echoes" (GNRE) throughout this paper.

¹Also at Department of Electrical Engineering, University of Western Ontario, London, Ontario, Canada.

Copyright 1997 by the American Geophysical Union.

Paper number 97JA00517.
0148-0227/97/97JA-00517\$09.00

In this paper we examine the characteristics of GNREs. We first describe the experiments from which our data sets were obtained. This is followed by a study of the properties of this new class of echoes. We show that GNREs have characteristics which differ significantly from the previously established scattering mechanisms for SuperDARN echoes (ground scatter and *E* and *F* region ionospheric backscatter) and present a detailed analysis which leads us to conclude that meteors are the source of these echoes. We end with a short discussion of the possibilities opened up by our finding.

2. Experiment

The SuperDARN radars were designed to study the convection patterns in the high-latitude ionosphere, patterns which can be mapped to the magnetosphere. These radars are pulsed HF radars operating in the frequency range ~9–15 MHz. Physically, each radar consists of a row of 16 log-periodic antennas which are directed approximately poleward. Owing to this physical antenna design, beam patterns are narrow ($\approx 4^\circ$) in the horizontal direction and broad ($\approx 30^\circ$) in the vertical direction, giving the beams a fan-like shape [Greenwald *et al.*, 1995]. The peak power is 10 kW, and the pulse width is 200–300 μ s, giving a range resolution of 30–45 km. Multilag autocorrelations are produced from which the power, Doppler velocity, and spectral width are calculated (see Greenwald *et al.* [1985] for an extensive discussion of the type of pulse sequence employed to obtain the autocorrelation functions). In the standard operating mode used for the collection of the data pre-

sented in this paper, the radar transmits successively for 6 s in each of 16 beam directions. The pulse sequence has a duration of about 40 ms, and each pulse sequence is separated from the next by 60 ms, giving 60 autocorrelation functions in each 6 s transmission; these are averaged together for each measurement. For a given range and beam, an average autocorrelation function (over 6 s) is obtained once every 100 s.

Most of the data used for the present study were taken at the Saskatoon radar (52.2°N, 106.5°W), although reference is also made to echoes received at Kapuskasing (49.4°N, 82.3°W). Other SuperDARN radars are located at Goose Bay (Canada), Iceland, Finland, and Halley Bay (Antarctica), with construction of additional sites in Iceland and Antarctica.

It will be shown that the GNREs have a scattering mechanism which depends on the neutral atmosphere. To help establish this dependence, we have made use of data from a second radar experiment, namely, the MF radar system at Saskatoon, which is dedicated to measurements of mesospheric winds by observations of vertical backscatter. This radar operates at 2.2 MHz and has a broad beam directed vertically. The height resolution of the MF radar is 3 km. The wind measurements are calculated by use of the full correlation analysis as described by *Manson and Meek* [1993].

Since we will be comparing observations from the Saskatoon MF and SuperDARN radars, it will be necessary to keep in mind that there is a significant spatial separation between the observing regions of the two radars. The MF Saskatoon beam is directed vertically, while the Saskatoon SuperDARN beam is directed northward. For the GNREs there is a spatial separation of 180 to 400 km. This separation may introduce some differences between observations from the two radars.

3. Characteristics of Grainy Near-Range Echoes

SuperDARN echoes are observed at near ranges, regardless of the amount of auroral activity. Typical examples of SuperDARN echo powers are presented in Figure 1. Figure 1a shows the range-time plot of echo power in beam 5 of the Saskatoon radar for October 21, 1994, which was a day of low magnetic activity K_p . The signals of interest for this paper show up clearly as a band of echoes at ranges of less than 400 km which can be seen throughout the entire 24 hours. On this magnetically quiet day these echoes can be seen extending to even greater ranges (600 or 700 km) for a few hours centered on 1200 UT. Figure 1b is from August 1, 1994, a day of moderate K_p . The GNREs are very similar to those in Figure 1a, but now there appear to be some E region auroral echoes also occurring at ranges less than 400 km. Nevertheless, the bulk of the echoes are still GNREs. Figure 1c is for September 8, 1994, a day of high K_p . Now the GNREs are obscured by auroral echoes over much of the time interval 0000 - 1000 UT,

and the strength of the GNREs is somewhat reduced compared to the Figures 1a and 1b (as are all other types of echoes). This decrease is most likely a result of enhanced D region ionization and the subsequent absorption of radio waves. The increase in low-altitude ionization levels has to be expected with an increase in precipitation energies at high K_p .

In Figures 1a-1c the GNREs show a smooth variation with time of day that contrasts with the patterns produced by the other types of echoes seen in this figure. For example, on October 21, 1994 at ranges between 1000 and 2000 km, there is a steady set of echoes due to ground backscatter from the F region. During a quiet day such as this the pattern of these echoes is largely controlled by the illumination of the ionosphere by the Sun. These echoes are also seen on August 1 (Figure 1b). The more structured and variable echoes seen at various ranges are due to backscatter from plasma irregularities in the E and F regions. In each case, when compared to the GNREs, these other types of echoes show much more variation from one day to the next and from one hour to the next on the same day.

The GNREs have a characteristic grainy or speckled appearance in Figures 1a-1c. In Figure 1d we examine 4 hours of the data for August 1, 1994 with expanded time and range scales. Each small rectangle in Figure 1d corresponds to one integration period (separated by 100 s in time) for one range gate (45 km in range). Evidently, the grainy appearance of the GNREs (range gates 500 km or less) arises from the seemingly random variation of the echo intensity from one integration period to the next and from one range to the next. This is distinctly different from the other types of echoes present in Figure 1. For those echoes there tends to be continuity in echo intensity over several integration periods and several successive ranges.

We conclude from Figure 1 that regardless of magnetic activity and its effects on the detection of auroral irregularities, the GNREs have a very steady day-to-day occurrence peaking around 1200 UT. This point is made more strongly in Figure 2, where we present the occurrence of near-range echoes (first five range gates from 180 to 400 km) as a function of universal time. The plot in Figure 2 shows the fraction of integration periods having echoes stronger than 10.0 dB above the noise level during each hour of local time for May 1994 (solid curve) and for October 1994 (dotted curve). In the data used for Figure 2 we have not attempted to separate GNREs from other types of echoes that may sometimes occur in this range interval.

For the 2 months shown in Figure 2, there was an occurrence peak in the morning hours (1200 UT \equiv 0600 LT), although with about a 2-hour delay in October compared with May. In both cases, the maximum echo percentage occurrence was about 50%. During the late afternoon the echo rate dropped to 10% (there still would be about four echoes/hour for each range bin). Similar diurnal patterns are observed for other months.

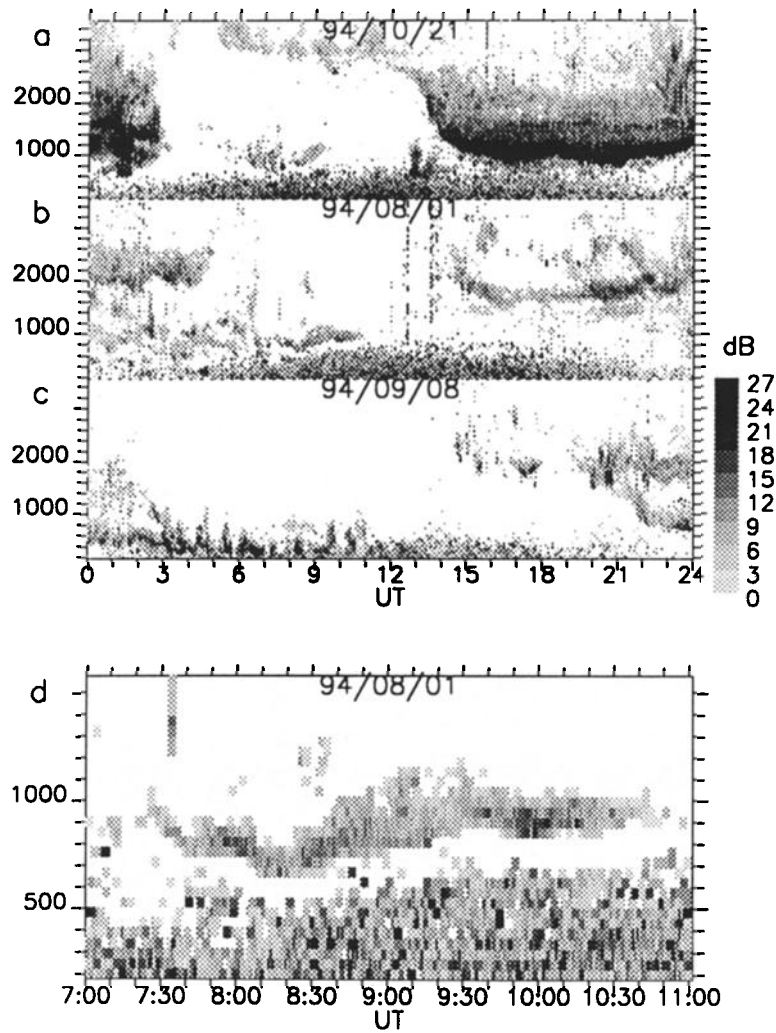


Figure 1. Range-time-intensity plots for beam 5 of Super Dual Auroral Radar Network (SuperDARN) Saskatoon from (a) October 21, 1994, (b) August 1, 1994, and (c) September 8, 1994. (d) Expanded section of Figure 1b. Note that the range scale starts at 200 km.

These diurnal patterns are also similar to the known behavior for meteors, including the variation from month to month in the time of the morning peak (J. Jones, private communication, 1997).

One can also notice the effect of strong meteor showers on the near-range echo powers. To help ensure that a meteor shower will show up in SuperDARN echoes, it is useful to find a shower whose radiant crosses the plane perpendicular to the SuperDARN beam. One shower that meets this requirement is the Geminid shower. It has a maximum occurring on December 13, 1993; for beam 5 of the Saskatoon SuperDARN radar the maximum flux is expected to occur over several hours either side of 0900 UT. The average power should be greater during the shower because at those times more of the integration periods will contain at least one meteor echo (the details of the way meteors would be detected by SuperDARN are discussed in a later section). In Figure 3 we show the daily variation in echo power during

the month of December 1993. For each day the power was averaged over the first five range gates and over the 4-hour interval of 0800 - 1200 UT, and divided by 10 times the average noise power (10 times noise is the conventional threshold used by the meteor radar community for meteor detection). The maximum which occurs on December 13 is almost 10 times more than the power observed on any other day of the month and corresponds exactly to the maximum of the Geminid shower for 1993.

The next radar echo property to consider is that of the Doppler velocity. Figure 4 shows the hourly averaged near-range Doppler velocities for August 1-8, 1994. While this plot has the usual amount of geophysical noise, it is readily apparent that the Doppler velocities have a strong and sometimes overwhelming semidiurnal component (see also Figure 7, bottom).

Another property of radar scatter which is commonly considered is the spectral width. The spectral width for

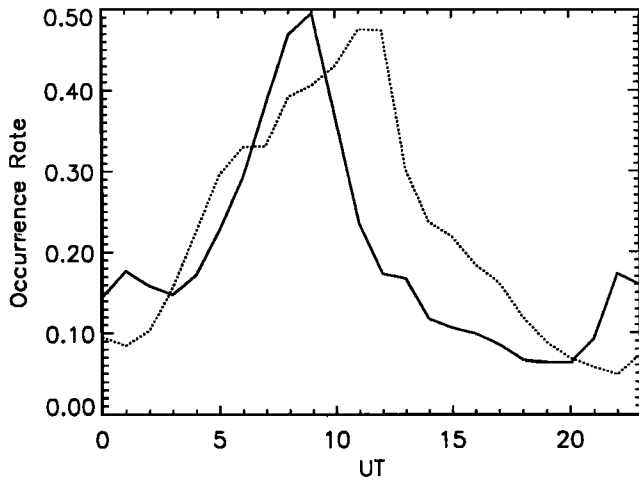


Figure 2. Mean daily occurrence of near-range echoes for May 1994 (solid curve) and October 1994 (dotted curve) for beam 5 of SuperDARN Saskatoon. This graph shows, for each hour, the fraction of integration periods containing echoes at least 10 dB above noise in the five nearest range gates, i.e., ranges between 180 and 405 km.

all SuperDARN echoes is obtained by curve fitting to the autocorrelation function power (see *Hanuise et al.* [1993] or *Villain et al.* [1996] for a more complete discussion of the fitting procedure). As shown in the histogram of spectral widths for April 1995 (Figure 5), the peak occurrence of spectral widths for the five nearest range gates is 4 ± 1 m/s while the mean spectral width is about 12 m/s.

4. Discussion

4.1. Origin of Grainy Near-Range Echoes

As a summary of section 3, we present in Table 1 the observed features of the SuperDARN GNREs, along

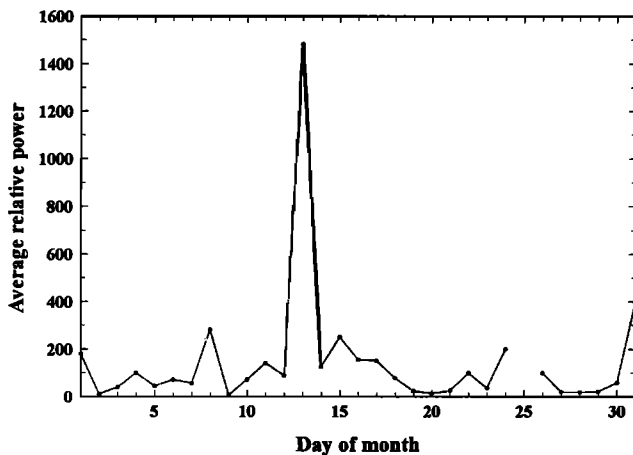


Figure 3. Power in beam 5 of SuperDARN Saskatoon for December 1993, averaged over the five nearest range gates between 0800 UT and 1200 UT for each day of the month, and measured relative to 10 times the average noise power.

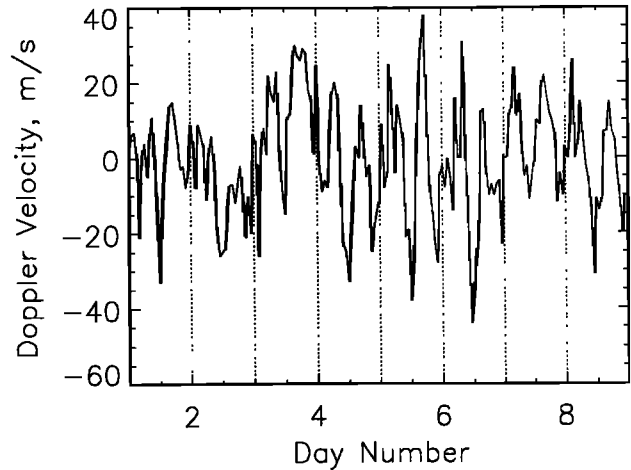


Figure 4. Hourly averaged Doppler velocities for 225 km range, beam 5 SuperDARN Saskatoon during August 1-8, 1994.

with known features of other common atmospheric and ionospheric echo types. Taken as a whole, the evidence overwhelmingly indicates that the GNREs are not due to an auroral scattering process but, instead, are due to some type of scatter which is related to the neutral atmosphere. The only candidates that we know of for such scatter are those shown in Table 1: scatter from meteors and MF scatter (the mechanism responsible for the mesospheric echoes obtained with MF radars).

The meteor scatter hypothesis is strongly supported by the graininess of the echoes (expected from the sporadic occurrence of meteors) and by the diurnal variation of the echoes (which matches that expected for meteor scatter). Even by themselves, these features provide convincing evidence against the MF scatter mechanism, but the direction of echoes expected for MF scatter appears to rule out that mechanism convincingly. All existing MF scatter experiments are carried

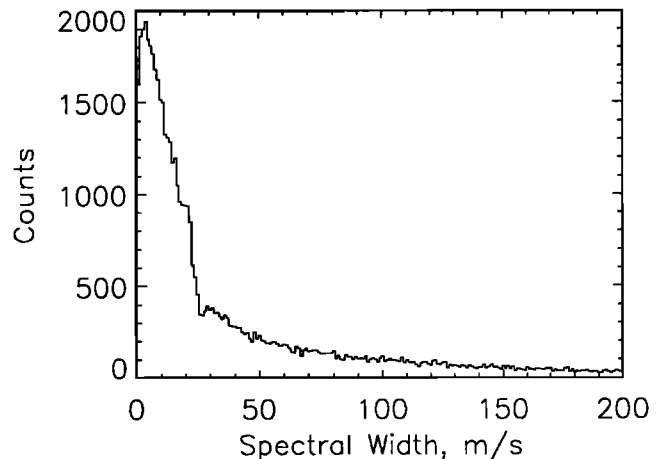


Figure 5. Histogram of spectral widths observed at Saskatoon during April 1995 for the five nearest range gates, beam 5.

Table 1. Characteristics of Atmospheric Radar Scatter

	SuperDARN GNRE*	Auroral E Region	Meteor Scatter	MF Scatter
		Occurrence		
Diurnal maximum	morning	night	morning	complex
Midday echoes	yes	no ^a	yes	yes
Meteor shower	yes	no	yes	uncertain
K_p dependence	no ^b	yes	no	modest
"Grainy" ^c	yes	no	yes	no
		Velocities		
Magnitude, m/s	≤ 50	≤ 500 at VHF	≤ 50	≤ 50
Dominant daily variation	semidiurnal	diurnal	semidiurnal	semidiurnal
Direction of elevation angle	near horizon	near horizon	any angle	near zenith

^aDuring very high K_p , auroral E region echoes could appear during midday at Saskatoon.

^bFor K_p values greater than 6, we find a decrease in GNRE power with K_p .

^cPrescription denotes large variations in echo power from one integration period to the next at a given range and from one range to the next for a given integration period.

*GNRE is grainy near-range echo.

out with vertically directed antennas, because experience has shown that MF scatter echoes are confined to a small range of directions about the zenith. For example, *Vincent and Belrose* [1978] studied the angular distribution of these echoes and were able to detect echoes only within 20° of the zenith. We know of no reports of MF scatter being detected at zenith angles as large as 60°. Because of the antenna pattern, the only range of zenith angles observable with the SuperDARN radars is 60° - 90°. We conclude that the MF scatter mechanism cannot be responsible for these near-range echoes. The evidence quite clearly supports the hypothesis that these echoes are due to backscatter from meteor trails.

In fact, radar echoes from meteor trails are a commonly observed feature of atmospheric radar echoes. Indeed, many systems are dedicated to making wind measurements by examining radar returns from meteor echoes [e.g. *Tsuda*, 1982; *Avery et al.*, 1990; *Nakamura et al.*, 1991].

4.2. Power and Spectral Measurements of Meteor Echoes With SuperDARN Radars

Although the evidence for meteor echoes as the origin of the GNREs is very strong, there are still several questions which need to be addressed. In particular, we need to understand how the backscatter power and spectral moments of meteor echoes from SuperDARN radars are to be interpreted, since the pulse coding and data processing used differ considerably from those of conventional meteor radars. First, a few details concerning meteor echoes will be useful. The radar signal is scattered from the trail of ionization left by the meteoroid as it passes through the atmosphere. If the electron density is sufficient to totally reflect the radar wave, the echo is said to be overdense. Overdense meteor echoes can be very strong and can last as long as

several seconds, but they are relatively rare. The majority of meteor echoes are underdense, and it can be shown that for such echoes the power P decays exponentially as the radius of the trail increases due to diffusion [e.g., *McKinley* 1961]:

$$P(t) = P_0 \exp\left(\frac{-t}{\tau}\right) \quad (1)$$

where the decay time constant τ is given by

$$\tau = \frac{\lambda^2}{32\pi^2 D} \quad (2)$$

where D is the diffusion coefficient in square meters per second and where λ is the radar wavelength.

The diffusion coefficient D increases with height, from about 3.0 m²/s near 90 km to over 20.0 m²/s around 100 km. (*McKinley* [1961] gives estimates of D based on early studies. We have updated these values using observations made by *Jones and Jones* [1990]). For the SuperDARN wavelength of 25 m, (2) gives values for the decay time constant in this height range of 0.6 s or less. This is considerably less than the 6-s integration period of the SuperDARN radar, but it is longer than the 40-ms duration of the pulse sequence used. Figure 6 illustrates the situation for one particular range gate for one 6-s integration period. The sixty 40-ms pulse sequences are indicated by the small rectangles along the time axis. The ordinate is received power in decibels above the noise level. An unnormalized autocorrelation function is calculated for each of the 60 pulse sequences, and these are averaged to give an average autocorrelation function for the integration period for this range gate. From this, the average power, mean Doppler velocity, and spectral width are estimated.

In Figure 6 we indicate echoes from three separate meteors. The echo labeled a has a line electron den-

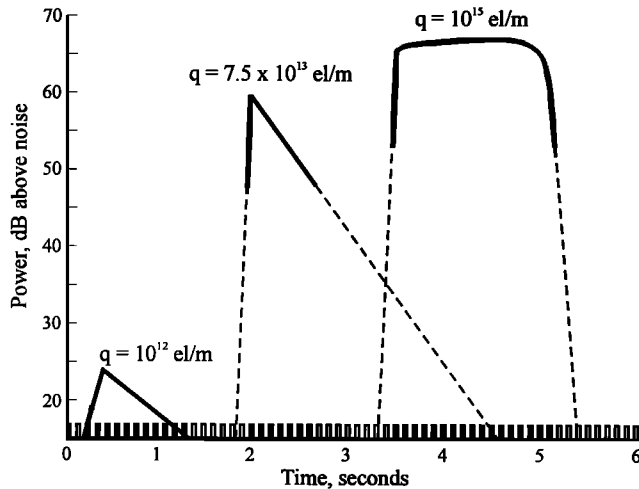


Figure 6. A sketch of one 6-s integration period, showing the 40-ms pulse sequences (rectangles), and three representative meteor echoes corresponding to trails with electron line densities of 10^{12} el/m (echo labeled a), 7.5×10^{13} el/m (echo b), and 10^{15} el/m (echo c).

sity of 10^{12} el/m and is estimated to be close to the threshold for SuperDARN, assuming a minimum signal-to-noise level of 10 dB, the criterion commonly used in the meteor radar community to define the minimum detectable meteor echoes (the peak of this echo is 24 dB above the noise level). This is an underdense meteor, so according to (1), the decay of the echo should appear as a straight line on a semilog plot. The risetime of the echo is determined by the speed of the meteoroid creating the ionization trail. For typical meteor speeds of 30 or 40 km/s this portion of the echo will last 100 - 200 ms. As drawn, the meteor echo from case a has a decay lifetime of 0.5 s, corresponding to an echo from a height of 91 km. By contrast, echo b in Figure 6 is close to the upper limit for underdense meteor trails, with a line density of 7.5×10^{13} el/m. It has been given a decay time constant of 0.15 s, corresponding to a height of 97 km. The power scattered by an underdense meteor is proportional to the square of the line density, so this second echo has an initial power which is 37 dB above that from the first. The solid portion of the curve shows the part of the echo contributing 90% of the total energy received in the echo. Echo c in Figure 6 has a line density of 10^{15} el/m and is overdense. Although the peak power is not much more than the strongest underdense echo, the total signal from this overdense echo is proportionately much larger because of the extended duration. These overdense meteors would completely dominate the observations except for the fact that smaller meteors are much more numerous than larger ones. In fact, the number of echoes with a line density greater than a particular value is inversely proportional to that value [Davies 1990]. Thus, for every meteor echo equal to or stronger than echo c in Figure 6 there will be about

13 equal to or stronger than echo b, and 1000 equal to or stronger than echo a.

Let us now consider how the data processing will deal with these meteor echoes. We will start by assuming that only echo a is present. For that case, 90% of the signal from the meteor echo will be found in pulse sequences 3 - 13 (indicated by solid shading in Figure 6); the remaining 54 sequences will return signals close to noise. A conventional spectral analysis (Fourier transform of the autocorrelation function) would produce a spectrum convolved with the 40 ms window of the pulse sequence, which would be dominated by the windowing. For this reason, in the SuperDARN spectral analysis a model is assumed for the spectral shape. By using a model, it is possible to fit the portion of the autocorrelation function which is measured and obtain an estimate of the spectral width which is not affected by windowing. The SuperDARN spectral analysis is routinely carried out assuming both Gaussian and Lorentzian spectral shapes. Except during the initial risetime (pulse sequences 3 and 4), which is a small part of the total signal, the pulse sequences will all sample the same exponential signal decay as given by (1). We expect the meteor trail to have the same line-of-sight velocity throughout its lifetime (under most circumstances, drifting with the neutral atmosphere); the mean Doppler shift of the echoes will be equal to that line-of-sight velocity and be the same for each of the pulse sequences. It follows that the autocorrelation function from each of the pulse sequences from the meteor echo should be the same except for amplitude. The average autocorrelation function for the integration period should also have that same shape. The average power for the integration period is given by the zero lag of the average autocorrelation function, which will be directly proportional to the sum of the powers of the meteor echo detected with the 11 pulse sequences (3 - 13) that lie within the duration of the echo. The Doppler shift inferred from the average autocorrelation function will be equal to the line-of-sight velocity of the meteor trail. Finally, the spectrum of an underdense meteor echo (equation (1)) is Lorentzian, so if we use the standard SuperDARN analysis with the Lorentzian model for the spectrum, we will get a good estimate of the spectral width associated with the meteor echo; but the spectral width of a meteor echo can be expressed in terms of the decay time constant τ :

$$\Delta v = \frac{\lambda}{4\pi\tau} \quad (3)$$

where Δv is the spectral width in Doppler units, and λ is the radar wavelength. Thus, for meteor echo a in Figure 6, with a decay time constant of 0.5 s, and assuming a wavelength of 25 m (frequency = 12 MHz), the spectral width would be 4 m/s, while for echo b the decay time constant of 0.15 s gives a spectral width of 12 m/s. We have chosen these particular decay time constants

on purpose, because the resulting spectral widths of 4 m/s (91 km altitude) and 12 m/s (97 km altitude) correspond to the mode and the mean of the distribution of spectral widths in Figure 5. Thus we have two estimates of the average heights at which the scattering is taking place.

Referring again to Figure 6, if both meteor echoes a and b are present during the same integration period, it is clear that the average autocorrelation function will be dominated by echo b; the power, mean Doppler velocity, and spectral width obtained from the signal analysis will be those of echo b. Most of the time, if there are two meteor echoes present, one of them will be larger than the other and the resulting autocorrelation function for the integration period will reflect the characteristics of only the stronger one. If any overdense meteor echo is present, such as echo c in Figure 6, it will completely dominate any underdense meteor echoes which may also be present, because it is both stronger and of longer duration. However, this situation will occur only occasionally, because there are relatively few overdense echoes. When there is an overdense meteor echo, the Doppler velocity inferred from the autocorrelation function would still be correct, but the spectral width will not be given by (3), as the variation of echo strength with time is no longer governed by the decay time constant. We might expect that such echoes, because of their long duration, would lead to unusually narrow spectral widths, and if interpreted as coming from an underdense meteor echo would imply an echo height much lower than the true height.

Next, we ask how often we might expect to observe more than one meteor echo in a given integration period and range gate. To answer that question, we need to know what the average meteor rate is. We can make a rough estimate of this from Figure 2. This shows that, on average, there is a probability of about 80% that a given range gate and integration period will have no meteor echoes. The number of meteor echoes in any one integration period should be governed by a Poisson distribution. A probability of 80% that there is no echo corresponds to an average meteor rate of 0.22 meteors per range gate per integration period. The probability of there being more than one echo in the same range gate is only 2%. At the maximum echo rate in Figure 2 there is about a 50% probability of no echo, and that corresponds to a meteor rate of 0.69 meteor echoes per range gate. There is then a probability of 12% that there will be two echoes in one range gate and 3% that there will be three echoes at one time. From these figures it is apparent that multiple echoes should be a relatively rare occurrence. The only exception to that statement might be during a meteor shower, when the echo rate could be significantly higher.

It would be helpful to know how often overdense meteor echoes are likely to occur, since, as noted above, the spectral width for such echoes does not give an esti-

mate of the height (through the decay time constant) as it does for underdense meteors. The transition to overdense meteors occurs at a line density of about 10^{14} el/m [Davies 1990]. Because of the inverse relationship between numbers of echoes and line density, there will be about 100 times as many meteor echoes above the SuperDARN radar threshold (line density of 10^{12} el/m) as there are overdense echoes. That is, about one in a hundred echoes will be overdense. This is an underestimate, because overdense echoes last sufficiently long that wind shear can distort a trail which is not initially perpendicular to the radar beam until it satisfies the condition for specular reflection. The magnitude of this effect is not easily estimated; it might increase the number of overdense meteor echoes by as much as a factor of 10, but overdense echoes should remain a small minority of the total number of echoes observed.

We also want to know if the number of GNREs observed is approximately equal to the number of meteor echoes to be expected with a radar such as SuperDARN. The average echo rate just calculated (0.22 meteors per range gate per integration period) corresponds to an hourly rate of 660 echoes/hour (GNREs are almost completely confined to five range gates, and the integration period is 6 s, so $0.22 \times 5 \times 3600/6 = 660$). We have compared this echo rate with an estimate obtained by comparing SuperDARN with a 32.7 MHz radar which was operated at Springhill (near Ottawa, Ontario) [Brown and Jones 1995]. Using the radar equation for meteor scatter applied to threshold conditions, the relative cosmic noise level at the two frequencies, and the known relation between meteor flux and electron line density and correcting for the effects of initial trail radius (the underdense "height ceiling" [McKinley, 1961]) and the characteristics of the two radars (much of the information on these points was provided by J. Jones (private communication, 1996)), we obtained an estimate that the SuperDARN flux should be about twice that of the Springhill radar. The average Springhill flux was about 200 echoes/hour, giving a SuperDARN estimate of about 400 echoes/hour. Considering all the uncertainties, this agrees well with the value of 660 echoes/hour estimated from Figure 2. We conclude that the observed SuperDARN meteor rate is about what should be expected.

4.3. Detailed Wind Velocity Comparisons

In this section, we will not consider near-range echoes for which the Doppler velocity magnitude is more than 200 m/s. This will largely eliminate from the analysis what few auroral radar echoes there might have been and the cases for which the velocities were poorly determined, leaving us with almost entirely GNREs.

As it appears that GNREs are scattered from meteor trails and since meteor trail winds are employed to measure the winds and waves in the middle atmosphere, it

is natural to compare the Doppler velocities measured for GNREs with the mesospheric winds measured by an MF radar at Saskatoon. The expectation is that the winds should match whenever they come from similar altitudes and that the best altitude for a comparison should match the average altitude at which meteor trails are produced. As an initial study, we considered just the wind component in the northward direction for this comparison, since this matches the average pointing direction of SuperDARN at Saskatoon.

In order to make statistical comparisons between the MF and SuperDARN velocities, one needs to compare longer sets of data and average the near-range echoes over the same hour which yields the MF radar measurements. Amplitude spectra for both the northward MF velocities at 97 km (Figure 7, top) and the beam

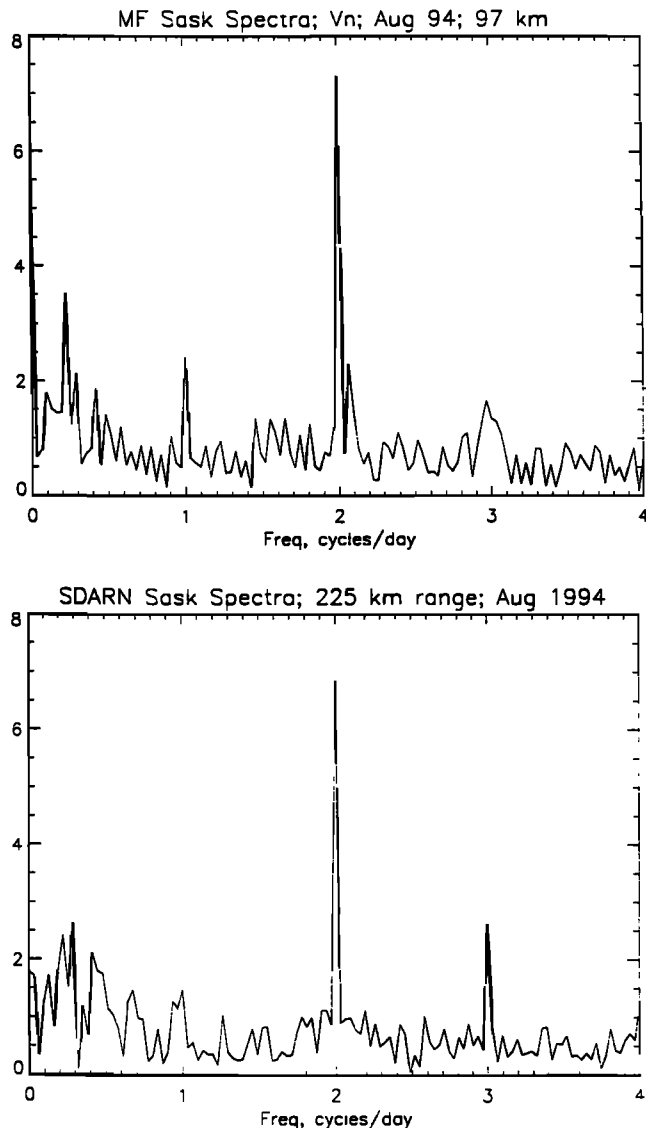


Figure 7. Amplitude spectra of winds during August 1994 for MF Saskatoon northward at (top) 97 km and (bottom) 225 km range, beam 5 of SuperDARN Saskatoon.

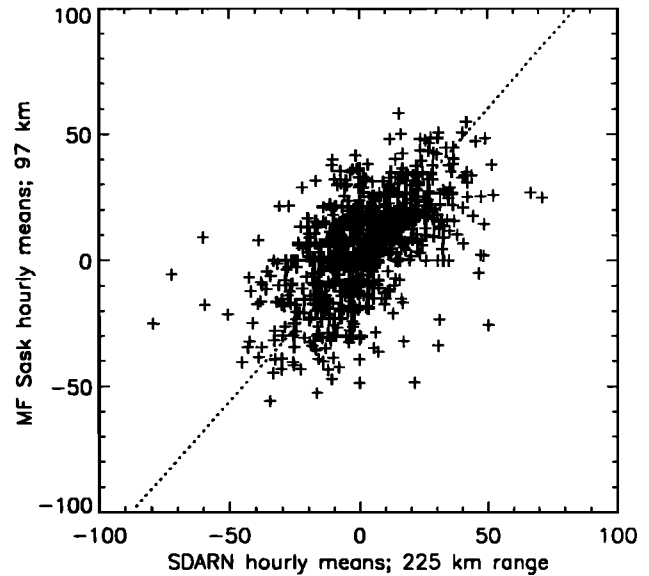


Figure 8. Scatterplot comparison of SuperDARN hourly means (225 km range, beam 5) and the MF velocities at 97 km for August 1994. The dotted line is the least squares fit $V_{MF} = (-2 \pm 1) + (1.16 \pm 0.06) \times V_{SDARN}$. The SuperDARN velocities have been rotated into the horizontal plane, and the MF velocities have been rotated into the SuperDARN azimuth direction.

5 SuperDARN velocities (Figure 7, bottom) are presented. The spectra, especially the peak at 2 cycles/day (semidiurnal oscillation) are most strikingly similar at this height. For further comparisons, the MF radar velocities in the east and northward directions were combined to yield the velocity in the SuperDARN azimuth direction (about 12° east of north). Also, noting that the SuperDARN velocities are radial rather than horizontal, we divided the velocities by the cosine of the vertical angle (obtained by assuming flat earth, 90 km height, and 225 km range). Figure 8 shows a scatterplot of the hourly mean wind measurements from MF (97 km) and SuperDARN Saskatoon (225 km range). The least squares best fit line was found to be

$$V_{MF} = (-2 \pm 1) + (1.16 \pm 0.06) \times V_{SDARN} \quad (4)$$

which is the dotted line in Figure 8. Thus, on average, the 97 km altitude MF velocities are about 16% greater than the SuperDARN velocities observed at the same time but at a location 200 to 300 km farther north. About 12% of this 16% difference can be explained by assuming that the dominant semidiurnal tide falls off, with latitude, as $\cos^2(\text{lat})$ [see Kato 1980, p. 71] and noting that the SuperDARN scattering point is 2.5° north of Saskatoon (52.2°N). This difference is consistent with variations in tides observed between comparably spaced MF radars [Hall et al., 1995]. Therefore, most of the small difference can be explained by this latitudinal effect. This result is at least as close as that found by other comparisons between meteor and MF

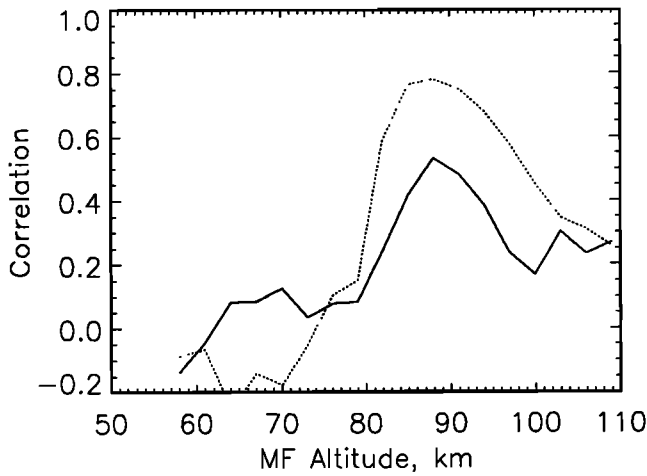


Figure 9. MF-SuperDARN velocity cross-correlation coefficient as a function of MF altitude for the month of January 1994 (solid curve) and August 1994 (dashed curve).

spaced antenna wind measurements [e.g., *Cervera and Reid, 1995*].

We also attempted to determine the altitude of the echoes from the height of the MF winds having the

strongest correlation with SuperDARN velocities. Figure 9 is a plot of the correlation of MF and SuperDARN wind as a function of height for the months of January 1994 (solid curve) and August 1994 (dashed curve). While the correlations shown in January 1994 are somewhat smaller than those found in August 1994, both comparisons show a good correlation which peaks for MF heights at 90 ± 10 km altitude. However, at higher altitudes the quantity of MF data becomes less and monochromatic gravity waves (often largely uncorrelated in characteristics over 500 km) become comparable to tides; both of these factors have the effect of shifting the height of best agreement to an altitude which is lower than the one where the data would be physically best correlated. Of these two factors, gravity waves may be predominant, since a comparison of hourly mean winds between MF radar and Fabry-Perot interferometer observations (both at Saskatoon) shows excellent agreement at ~ 97 km [*Manson et al., 1997*].

A third way of using MF data to determine the altitude of the GNRE echoes is to compare the phases of the semidiurnal tidal oscillations. In Figure 10 we show the mean day northward velocities for both the SuperDARN near-range echoes (five nearest ranges, filtered to

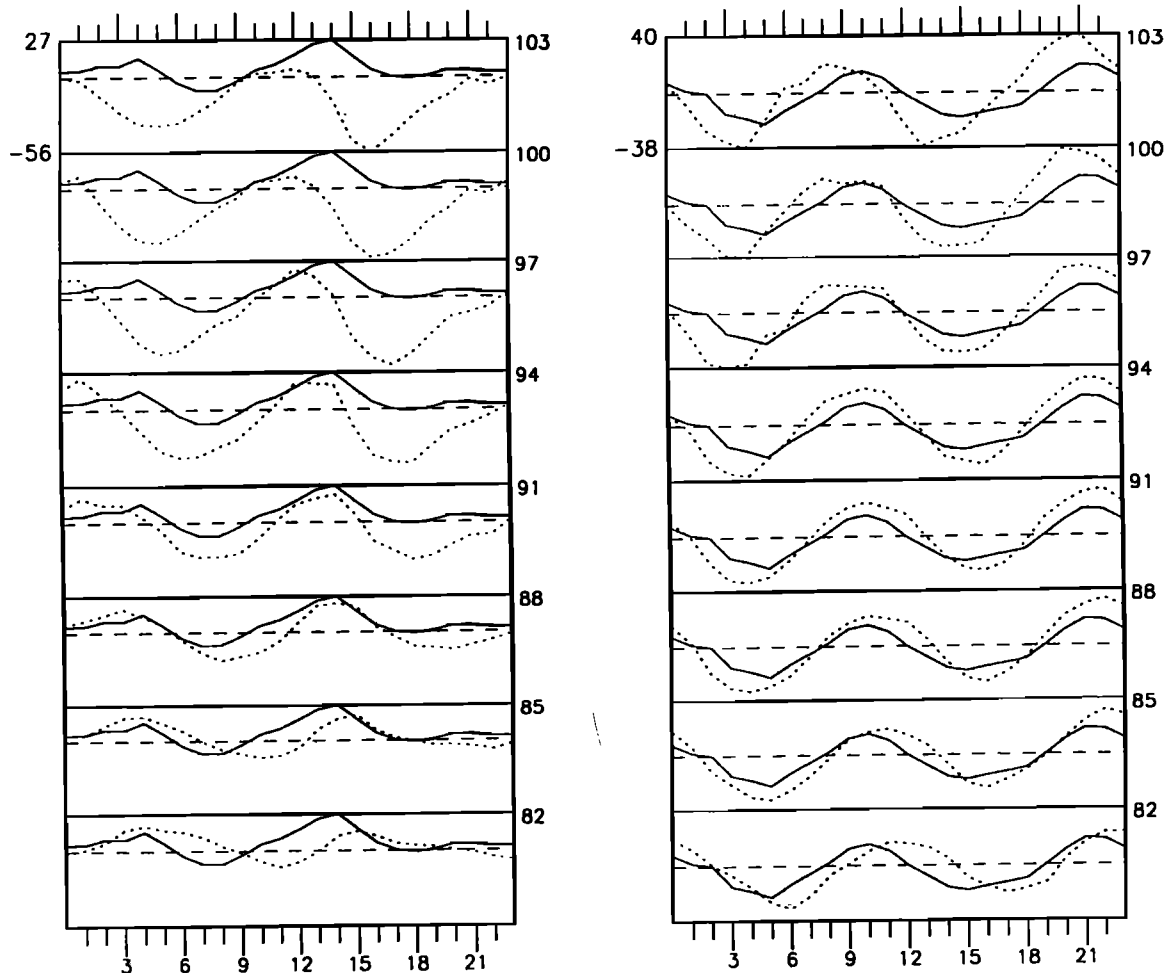


Figure 10. Mean day velocities for SuperDARN for the five nearest ranges, beam 5 (solid curves) and MF Saskatoon for heights from 82-103 km (dotted curves) for (left) August 1994 and (right) September 1994.

remove nonmeteor echoes, shown as solid curves), and for the MF Saskatoon data (dotted curves) for a range of heights from 82 to 103 km (numbers at the right). The dashed line for each plot shows zero velocity, and the velocity scales in meters per second are indicated by the numbers at the top left of each panel. Figure 10 (left) shows the mean day for January 1994, while Figure 10 (right) shows the data for September 1994. For both of these months and in general, the wind pattern is dominated by the strong semidiurnal oscillation. In Figure 10 the phase shift of the semidiurnal oscillation in the MF mean day velocities can be seen to change with altitude and to agree with that of the SuperDARN observations at a particular height, 91 km for January 1994 and 94 km for September 1994. Quantitative estimates of the height were obtained by plotting against MF height the relative MF-SuperDARN phase shift of the semidiurnal component and then determining the height at which this relative phase shift was zero. This method of comparison cannot be used for all months of the year, because at times, especially in the summer [Fellous *et al.*, 1975; Manson and Meek, 1986], there is very little variation of the phase of the semidiurnal tide with height in the 80 - 100 km region. We made this comparison on data from 6 of the 12 months in 1994 and obtained an average height of 94 ± 3 km.

4.4. Scatterer Height Determination

The value of the SuperDARN radar as a meteor wind system will be enhanced by having estimates of the altitude of the echoes. Table 2 summarizes the heights obtained by the different measurements considered in this study.

The first three entries in Table 2 (a, b, and c) are based on the comparisons we just made between the MF winds and the SuperDARN Doppler velocities. As mentioned earlier, the cross-correlation of hourly values (Figure 9) tends to produce lower heights due to the lesser quantity of MF data and the decorrelating effects of gravity waves at the upper altitudes. As for the spectral comparison (Figure 7), it suffers from the qualitative nature of the comparison; we visually picked the heights where the features matched most satisfactorily. Of the three MF-SuperDARN comparisons, we consider the most reliable one to be that obtained from

the tidal phase variation with altitude (Figure 10) which produced height estimates of 94 ± 3 km.

For the fourth altitude determination (entry d in Table 2) we have used vertical interferometry results. The work was undertaken by D. André from the University of Saskatchewan, who determined that the echo heights for the near-range echoes had to be between 80 and 100 km (D. André, private communication, 1996). Note that using long data sets, it should be possible to greatly improve the accuracy of this measurement.

The final two entries in Table 2 come from the relation between spectral width and decay time constant, assuming that the meteor echoes are predominantly underdense. As mentioned earlier, from the histogram of widths (Figure 5), we obtained a peak spectral width of 4 m/s (corresponding to a height of 91 ± 2 km) and a mean width of 12 m/s (97 ± 2 km height). In summary, we conclude that all the height determinations are consistent with meteor scatter coming, on average, from an altitude of 94 ± 3 km.

It is not at all straightforward to compare the heights in Table 2 with what would be expected from meteor echoes, because of several systematic effects. As mentioned earlier, many of the height distributions found in the literature for radar meteors are affected by the underdense height ceiling [McKinley, 1961], a consequence of the finite initial trail radius. The height ceiling is a strong function of radar wavelength, so ideally, we would compare our SuperDARN heights with results from a meteor radar operating at the same frequency. There do not appear to have been any height studies at 25 m wavelength, but McKinley [1961] reports a study made by Greenhow at 17 m wavelength, which found an approximately Gaussian distribution with a maximum at 102 km and a standard deviation of about 7 km. This cannot be compared directly with SuperDARN heights because of another systematic effect which is peculiar to SuperDARN observations. The signal-to-noise (SNR) of an underdense meteor echo is proportional to the integral of the backscattered power (equation (1)) over the 6-s integration period. Since the decay time constant τ is typically much less than the integration time, that means that the SNR is proportional to $P_0\tau$; but τ decreases with increasing height, so a particular SNR threshold corresponds to larger values of P_0 (elec-

Table 2. Summary of SuperDARN Near Range Echo Height Measurements

Measurement	Source of Estimate	Height, km
a	cross-correlation with Saskatoon MF	80-100
b	spectral comparison with Sask MF	94-106
c	phase of semi-diurnal tide	94 ± 3
d	vertical angle measurement	80-100
e	spectral width using peak of Fig. 5	91 ± 2
f	spectral width using mean of Fig. 5	97 ± 2

tron line densities) for greater heights. In other words, SuperDARN sees a smaller fraction of the meteors at greater heights. For a Gaussian height distribution this effect can be treated analytically; applying it to the Greenhow distribution is found to lower the height of the distribution by 7 km to an average height of 95 km, in good agreement with the results in Table 2.

5. Summary

The SuperDARN radars observe grainy near-range echoes (GNREs) on a daily basis. These are unaffected by varying magnetic disturbance (except for events with anomalous D region absorption). It has been found that the Doppler velocities of these echoes are strongly semidiurnal and are in agreement with the winds measured by an MF radar in the upper atmosphere. The spectral widths were found to be in excellent agreement with meteor trail diffusion at the same altitudes. All the height determinations, both directly through vertical interferometry and indirectly through comparisons of winds by diffusion time calculations, agreed with a height of 94 ± 3 km, close to the average height expected for meteor echoes. The graininess of these echoes (random variation of echo intensity from one range gate or integration period to the next) is the temporal and spatial behavior expected of backscatter from meteor trails. The rate of occurrence of GNREs is found to correspond closely to the number of meteor echoes predicted for a radar with SuperDARN characteristics, and the backscatter power of GNREs is found to increase at times of meteor showers. We therefore conclude that these grainy near-range SuperDARN echoes (constituting the majority of near-range echoes) are due to meteor trails.

The meteor trail hypothesis allows us to understand why the short-range echoes are so distinctly narrow, why the Doppler shifts are of the order of 50 m/s or less, why the frequency of occurrence of the near-range echoes peaks in the early morning hours, and also why the observed Doppler shifts are particularly well correlated with mesospheric winds measured by MF radars.

The existence of a strong meteoritic component in SuperDARN near-range echoes may have some serious consequences for our understanding of auroral echoes. For instance, *Eglitis et al.* [1995] have recently compared histograms of HF and VHF radio spectra at close range. While they noticed that the HF spectra were different from the VHF spectra in many ways, they treated all near-range HF echoes as if they were produced by plasma turbulence. This made the HF plasma turbulence processes look quite different from what is observed at higher frequencies. However, once it is recognized that the bulk of near-range HF spectra in that study may well have been meteor echoes, we then find a simple explanation for the otherwise puzzling differences. For this conclusion to hold, the contamination of the results by meteor scatter should be much less of

a problem at VHF frequencies than it is at HF. Indeed, this is known to be true. Several different frequency-dependent effects (noise level, initial meteor trail radius, frequency dependence of scattering cross section) combine to reduce the signal-to-noise ratio with increasing frequency. We are currently attempting to study the properties of "real" HF radar auroral spectra by seeking a way to separate meteor echoes from the auroral echoes.

This same process of separating meteor and auroral echoes will help us to use the meteor echoes detected by the SuperDARN radars for the study of high-latitude mesospheric winds, at least at times when the effects of strong electric fields are not severe [Reid, 1983]. The widespread spatial distribution of the SuperDARN radars will make this network a valuable tool for the study of these winds on a global scale. Because of the spread in the heights of SuperDARN meteor echoes, SuperDARN data will be most useful for the study of atmospheric modes with relatively long vertical wavelengths, such as the semidiurnal and 2-day components.

Acknowledgments. We acknowledge helpful discussions with D. André, P. Brown, and J. Jones. This research was supported by grants from the Natural Sciences and Engineering Research Council of Canada. The funds for the Saskatoon HF radar and for the support of the first author (G.E.H.) were provided by NSERC CSP grant 119615 for "The Canadian Component of SuperDARN".

The Editor thanks R. G. Roper and S. Palo for their assistance in evaluating this paper.

References

- Avery, S. K., J. P. Avery, T. A. Valentic, S. E. Palo, M. J. Leary, and R. L. Obert, A new meteor detection and collection system: Christmas Island mesospheric wind measurements, *Radio Sci.*, **25**, 657-669, 1990.
- Brown, P., and J. Jones, A determination of the strengths of sporadic radio-meteor sources, *Earth, Moon Planets*, **68**, 223-245, 1995.
- Cervera, M. A., and I. M. Reid, Comparison of simultaneous wind measurements using colocated VHF meteor radar and MF spaced antenna radar systems, *Radio Sci.*, **30**, 1245-1261, 1995.
- Davies, K., *Ionospheric Radio Propagation* Peter Peregrinus, London, 1990.
- Eglitis, P., T. R. Robinson, I. W. McCrea, K. Schlegel, T. Nygren, and A. S. Rodger, Doppler spectrum statistics obtained from three different-frequency radar auroral experiments, *Ann. Geophys.*, **13**, 56-65, 1995.
- Fellous, J. L., R. Bernard, M. Glass, M. Masseur, and A. Spizzichino, A study of the variations of atmospheric tides in the meteor zone, *J. Atmos. Terr. Phys.*, **37**, 1511-1524, 1975.
- Greenwald, R. A., K. B. Baker, R. A. Hutchins, and C. Hanuise, An HF phased-array radar for studying small-scale structure in the high-latitude ionosphere, *Radio Sci.*, **20**, 63-79, 1985.
- Greenwald, R.A., et al., DARN/SUPERDARN: A global view of the dynamics of high-latitude convection, *Space Sci. Rev.*, **71**, 761-796, 1995.
- Hall, G. E., S. P. Namboothiri, A. H. Manson, and C. E. Meek, Daily tidal, planetary wave, and gravity wave am-

- plitudes over the Canadian prairies, *J. Atmos. Terr. Phys.*, *57*, 1553-1567, 1995.
- Hanuse, C., J. P. Villain, D. Grésillon, B. Cabrit, R. A. Greenwald, and K. B. Baker, Interpretation of HF radar ionospheric Doppler spectra by collective wave scattering theory, *Ann. Geophys.*, *11*, 29-39, 1993.
- Jones, W., and J. Jones, Ionic diffusion in meteor trails, *J. Atmos. Terr. Phys.*, *52*, 185-191, 1990.
- Kato, S., *Dynamics of the Upper Atmosphere*, Cent. for Acad. Pub., Tokyo, 1980.
- Manson, A. H., and C. E. Meek, Dynamics of the middle atmosphere at Saskatoon (52°N, 107°W): A spectral study during 1981, 1982, *J. Atmos. Terr. Phys.*, *48*, 1039-1055, 1986.
- Manson, A. H., and C. E. Meek, Characteristics of gravity waves (10 min-6 hours) at Saskatoon (52°N, 107°W): Observations by the phase coherent medium frequency radar, *J. Geophys. Res.*, *98*, 20,357-20,367, 1993.
- Manson, A. H., F. Yi, G. Hall, and C. E. Meek, Comparisons between instantaneous wind measurements made at Saskatoon (52°N, 107°W) using colocated MF radars and FPI instruments: Climatologies 1988-1992 and case studies, *J. Geophys. Res.*, in press, 1997.
- McKinley, D.W.R., *Meteor Science and Engineering*, McGraw-Hill, New York, 1961.
- Nakamura, T., T. Tsuda, and M. Tsutsumi, Meteor wind observations with the MU radar, *Radio Sci.*, *26*, 857-869, 1991.
- Reid, G., The influence of electrical fields on radar measurements of winds in the upper mesosphere, *Rad. Sci.*, *18*, 1028-1034, 1983.
- Tsuda, T., Kyoto meteor radar and its application to observation of atmospheric tides, Ph.D. thesis, Radio Atmos. Sci. Cent., Kyoto Univ., Japan, January 1982.
- Villain, J. P., R. André, C. Hanuse, and D. Grésillon, Observation of the high latitude ionosphere by HF radars: Interpretation in terms of collective wave scattering and characterization of turbulence, *J. Atmos. Terr. Phys.*, *58*, 943-958, 1996.
- Vincent, R. A., and J. S. Belrose, The angular distribution of radio waves partially reflected from the lower ionosphere, *J. Atmos. Terr. Phys.*, *40*, 35-47, 1978.

G.E. Hall, D.R. Moorcroft, and J.-P. St.-Maurice Department of Physics and Astronomy, University of Western Ontario, London, Ontario, Canada N6A 3K7. (e-mail: hall@danlon.physics.uwo.ca)

J. W. MacDougall, Department of Electrical Engineering, University of Western Ontario, London, Ontario, Canada N6A 3K7. (e-mail: macdougall@danlon.physics.uwo.ca)

A.H. Manson and C.E. Meek, Institute of Space and Atmospheric Studies, University of Saskatchewan, Saskatoon, Saskatchewan, Canada, S7N 0W0 (e-mail: manson@dansas.usask.ca)

(Received February 13, 1996; revised February 12, 1997; accepted February 17, 1997.)